Title: Impaired AMPA receptor activation directly triggers homeostatic synaptic scaling
Last Revised: 2013-July-05 at 13:45 (MF)
Author Names: Ming-fai Fong, Jonathan P. Newman, Steve M. Potter, Peter Wenner
Intended Journal: Nature (letter format)

Mechanisms of homeostatic plasticity are thought to help foster stable activity in developing neural circuits. One well-studied form of homeostatic plasticity is synaptic scaling, a phenomenon in which the quantal amplitudes of all synaptic inputs onto a neuron are strengthened (upscaling) or weakened (downscaling) by a multiplicative factor to compensate for chronic changes in activity levels (Turrigiano, 2012). Synaptic upscaling is commonly elicited through prolonged pharmacological suppression of spiking or excitatory synaptic transmission. Because suppression of spiking reduces AMPA receptor (AMPAR) activation, and suppression of AMPAR activation reduces spiking, it has been difficult to distinguish between the effects of reduced spiking and reduced transmission in triggering upscaling (Rich and Wenner, 2007; Vitureira et al., 2011). Here we use a combination of multisite electrophysiology, optogenetics, and pharmacology to separate the roles of spiking and AMPAergic transmission on synaptic scaling. We show that chronic suppression of AMPAergic transmission triggers upscaling even when spiking activity is restored to normal levels. We also show that upscaling triggered by spiking activity blockade can be significantly attenuated by partial restoration of AMPAR activation. Together these results demonstrate that upscaling of excitatory synapses is triggered by reductions in AMPAR activation rather than reductions in spiking activity. Our findings suggest that the function of synaptic upscaling may be for compensatory regulation of synaptic strength rather than as a means of homeostatically controlling neuronal spiking activity.

Neurons are thought to tightly regulate their spiking activity through compensatory changes in synaptic strength and intrinsic cellular excitability. Although homeostatic synaptic

scaling has been observed in many different systems (Davis, 2006), it is unclear how perturbations to spiking activity trigger scaling. It is often assumed that blocking voltage-gated Na^+ channels with TTX (tetrodotoxin) or AMPARs with CNQX (6-cyano-7-nitroquinoxaline-2,3-dione) both block spiking activity, which then triggers upscaling. To test this assumption we used a planar microelectrode array (MEA; Fig. 1a-b) to continuously record extracellular spiking from hundreds of neurons embedded in dissociated cortical cultures during 24-hour TTX or CNQX application to examine the changes in spiking activity that are thought to lead to upscaling. We used the MEA recordings to detect network-wide bursts of action potentials occurring synchronously across many electrodes (hereafter referred to as bursts) and to assess a culture's overall firing rate by summing spiking levels throughout the array (Fig. 1c, Wagenaar et al., 2006).

Consistent with our expectations, blockade of TTX eliminated spiking activity for the entire 24-hour treatment (Fig. 1d-e). However, we found that CNQX only partially reduced spiking activity compared to pre-drug levels (Fig. 1d-e). The CNQX-induced reduction in firing rate was primarily due to a reduction in burst frequency (Fig. 1f). Meanwhile, spiking between bursts was not significantly affected (Fig. 1f). In most CNQX-treated cultures, bursting was significantly reduced during the first few hours, but began to recover by the end of 24 hours (Fig. 1d). While the reduction in activity following CNQX was variable across cultures, some degree of spiking and bursting always persisted, unlike those treated with TTX.

We hypothesized that cultures experiencing greater reductions in spiking activity might also experience more dramatic upscaling of miniature excitatory postsynaptic currents (mEPSCs). To test this hypothesis, we used whole-cell recordings to measure mEPSCs from

pyramidal cells following 24-hour application of TTX or CNQX (Fig. 2a-b). Consistent with previous literature (Turrigiano et al., 1998; Jakawich et al., 2010), chronic TTX or CNQX both produced similar increases in mEPSC amplitude over vehicle-treated sister control cultures (Fig. 2c, f; TTX, 146.81±7.98% of control; CNQX, 142.94±4.49% of control) and showed the scaling profile (Fig. 2d-e, g-h). This indicated that cells from cultures experiencing only moderate reductions in spiking scaled equally to cells that experienced complete elimination of spiking. To further explore the relationship between spiking and scaling, we compared changes in spiking and mEPSC amplitude for individual sister culture pairs. For each culture, we compared the reduction in MEA-recorded firing rate during the 24-hour TTX or CNQX application to the increase in mean mEPSC amplitude recorded following the treatment (Fig. 2i). We observed no correlation between the TTX- or CNQX-induced change in firing rate and the resultant increase in mEPSC amplitude (r = -0.0466). Moreover, we could not find a relationship between the increase in mEPSC amplitude and any other features of spiking activity (Fig. 2i; burst rate, r = 0.1136; interburst firing rate, r = 0.0435). Overall, the lack of correlation between spiking and scaling raise the possibility that reduced spiking activity does not trigger upscaling.

Instead of reduced spiking activity, it is possible that reductions in AMPAR activation might directly trigger scaling. It has been difficult to distinguish between the independent effects of spiking and AMPAR activation on synaptic scaling because they are highly-coupled processes. Since TTX and CNQX each reduce both spiking and AMPAR activation, either directly or indirectly, there are several possibilities for what activity signal could be triggering synaptic scaling: [I] reductions in spiking alone, [II] reductions in AMPAR activation alone, [III]

concurrent reductions in both spiking and AMPAR activation, or [IV] reductions in either spiking or AMPAR activation.

In order to examine the effects of reducing AMPAR activation while leaving spiking intact, we developed a closed-loop optical stimulation system for restoring the normal levels of spiking activity during a 24-hour application of CNQX (Fig. 3a; Newman et al., in prep). We transfected neurons with channelrhodopsin-2 (ChR2) and observed expression throughout the culture within a week (Fig. 3b). Because the reduction in spiking following CNQX application is primarily due to a reduction in network-wide bursts (Fig. 1f), we selected a stimulation strategy that favored reinstatement of bursting. Brief pulses of blue light (10 ms, 465 nm, 5 $mW \cdot mm^{-2}$) effectively reproduced spontaneous-like bursts in the presence of CNQX (Fig. 3c-d, Suppl. Fig. 3). Although each stimulus produced some short latency spikes that resulted directly from ChR2 activation, the vast majority of spikes were contained in longer latency barrages that occurred after the light pulse terminated. These longer latency barrages of spikes closely matched spontaneously-occurring bursts in terms of time course and profile of network recruitment of (Fig. 3c-d), and are presumably dependent on NMDAergic transmission (Suppl. Fig. 4). To precisely control firing rate at a particular setpoint, the timing of each stimulation pulse was determined in real-time based on spiking activity recorded through the MEA (Newman et al., in prep). In order to restore normal levels of spiking during an AMPAR blockade, we treated cultures with CNQX and began closed-loop optical stimulation with a target spiking level set to the pre-drug firing rate (Fig. 3e). Closed-loop optical stimulation effectively restored control firing and burst rates (Fig. 3e-g).

We recorded mEPSCs from triplicate sister cultures: [1] vehicle-treated control cultures experiencing normal AMPAR activation and normal spiking activity, [2] CNQX-treated cultures experiencing no AMPAR activation and reduced spiking, and [3] photostimulated CNQX-treated cultures experiencing no AMPAR activation but restored spiking activity (Fig. 3h). We found that stimulated and unstimulated CNQX-treated cultures had mEPSC amplitudes that were elevated over sister control cultures (Fig 3i) and showed a scaled distribution (Fig. 3j-k). Further, we found that the mean and distribution of mEPSC amplitudes were virtually identical in AMPAR-blocked sister cultures regardless of whether they experienced reduced or normal levels of spiking activity (Fig. 3j-k; $P>0.9$). The results demonstrate that upscaling associated with AMPAR blockade is not triggered by reductions in spiking or spike-dependent processes (e.g. burst depolarizations, activation of voltage-gated calcium channels - VGCCs and consequent calcium signaling/presynaptic release). Therefore, reduced AMPAR activation by itself can trigger scaling, and reduced spiking is not necessary for upscaling (eliminates possibility I & III).

Based on our observation that reduced AMPAR activation can independently trigger scaling, we might expect that blocking activity with TTX triggers scaling because it reduces spike-dependent release of neurotransmitter, and therefore reduces AMPAR activation. We therefore tested the importance of reduced AMPAR activation in TTX-treated cultures by restoring some AMPAR activation during TTX treatment. We used the AMPAR modulator, cyclothiazide (CTZ), to increase the amplitude and frequency of mEPSCs during TTX treatment (Fig. 4a), and these effects lasted for at least 12 hours (Suppl. Fig. 6). Like TTX, co-treatment of cultures with TTX and CTZ completely abolished spiking activity (Suppl. Fig. 7). The amplitude

of mEPSCs recorded from cultures following 24-hour application of TTX and CTZ were significantly reduced compared to those treated with TTX alone (Fig. 4c). A multiplicative relationship between amplitude distributions existed for all 3 conditions (Figure 4d-e, Fig. 2e). These results demonstrate that partially restoring AMPAR activation during a spiking blockade reduces the upscaling observed following chronic TTX treatment. Together, the results suggest that upscaling after TTX or CNQX are both triggered by reductions in AMPAR activation (possibility II), rather than reduced spiking activity (possibility I or IV).

Current thinking in the field suggests that reductions in somal action potentials (APs) lead to reduced VGCC opening and subsequent reductions in global calcium signaling, which then trigger the upscaling of AMPAergic quantal amplitude (Turrigiano, 2012). This would provide an elegant method for the homeostatic control of a cell's spiking activity. However, our results do not support this model. First, upscaling still occurred when somal APs were restored during AMPAR blockade; second, upscaling was attenuated when AMPAR activation was partially restored while somal APs were eliminated. Rather, our results suggest upscaling is mediated by reduced AMPAR activation, and that any downstream calcium signaling that mediates it will be initiated locally in the dendrite as scaling was influenced by altering AP-independent quantal currents (CTZ and TTX). The spike-dependent model of upscaling is based on a study that blocked somal spiking and demonstrated an accumulation of AMPARs within hours (Ibata, Sun et al. 2008). Reasons for the differences between our study and that of Ibata et al. could be due to the method of scaling measurements (mEPSC amplitude vs. expression of AMPARs) or timing of the scaling process (24 hours vs. 3 hours). On the other hand, our observation that reductions in spiking alone are insufficient to trigger upscaling is consistent with

previous *in vitro* and *in vivo* studies showing that chronic reductions of spiking in single cells with unperturbed synaptic inputs did not increase mEPSC amplitude (Burrone et al., 2002; Pratt and Aizenman, 2007). Further, our finding that local synaptic signaling triggers compensatory changes in AMPAergic synaptic strength is consistent with a number of previous studies. These studies have shown that when receptor activation is chronically reduced at specific synapses, compensatory changes occur only at those synapses experiencing lowered transmission (Hou et al., 2008; Beique et al., 2011; Deeg and Aizenman, 2011; Sutton et al., 2006; Jakawich et al., 2010). Our finding that receptor activation triggers cell-wide synaptic scaling raises the possibility that upscaling of mEPSC amplitudes is merely the result of reducing AMPAergic transmission throughout the cell and therefore triggering local synaptic compensations at all synapses. This would suggest that upward scaling has little to do with homeostatic control of a cell's spiking activity, but instead is a transmission-dependent plasticity that facilitates local maintenance of synaptic strength.

References

Beique JC, Na Y, Kuhl D, Worley PF, Huganir RL (2011) Arc-dependent synapse-specific homeostatic plasticity. Proc Natl Acad Sci U S A 108:816-821.

Burrone J, O'Byrne M, Murthy VN (2002) Multiple forms of synaptic plasticity triggered by selective suppression of activity in individual neurons. Nature 420:414-418.

Davis, G. W. (2006). "Homeostatic control of neural activity: from phenomenology to molecular design." Annu Rev Neurosci **29**: 307-323.

Deeg KE, Aizenman CD (2011) Sensory modality-specific homeostatic plasticity in the developing optic tectum. Nat Neurosci 14:548-550.

Hou Q, Zhang D, Jarzylo L, Huganir RL, Man HY (2008) Homeostatic regulation of AMPA receptor expression at single hippocampal synapses. Proc Natl Acad Sci U S A 105:775-780.

Ibata K, Sun Q, Turrigiano GG (2008) Rapid synaptic scaling induced by changes in postsynaptic firing. Neuron 57:819-826.

Jakawich SK, Nasser HB, Strong MJ, McCartney AJ, Perez AS, Rakesh N, Carruthers CJ, Sutton MA (2010) Local presynaptic activity gates homeostatic changes in presynaptic function driven by dendritic BDNF synthesis. Neuron 68:1143-1158.

Pratt KG, Aizenman CD (2007) Homeostatic regulation of intrinsic excitability and synaptic transmission in a developing visual circuit. J Neurosci 27:8268-8277.

Rich MM, Wenner P (2007) Sensing and expressing homeostatic synaptic plasticity. Trends Neurosci 30:119-125.

Sutton MA, Ito HT, Cressy P, Kempf C, Woo JC, Schuman EM (2006) Miniature neurotransmission stabilizes synaptic function via tonic suppression of local dendritic protein synthesis. Cell 125:785-799.

Turrigiano G (2012) Homeostatic synaptic plasticity: local and global mechanisms for stabilizing neuronal function. Cold Spring Harb Perspect Biol 4.

Turrigiano GG, Leslie KR, Desai NS, Rutherford LC, Nelson SB (1998) Activity-dependent scaling of quantal amplitude in neocortical neurons. Nature 391:892-896.

Vitureira N, Letellier M, Goda Y (2011) Homeostatic synaptic plasticity: from single synapses to neural circuits. Curr Opin Neurobiol.

Wagenaar DA, Pine J, Potter SM (2006) An extremely rich repertoire of bursting patterns during the development of cortical cultures. BMC Neurosci 7:11.

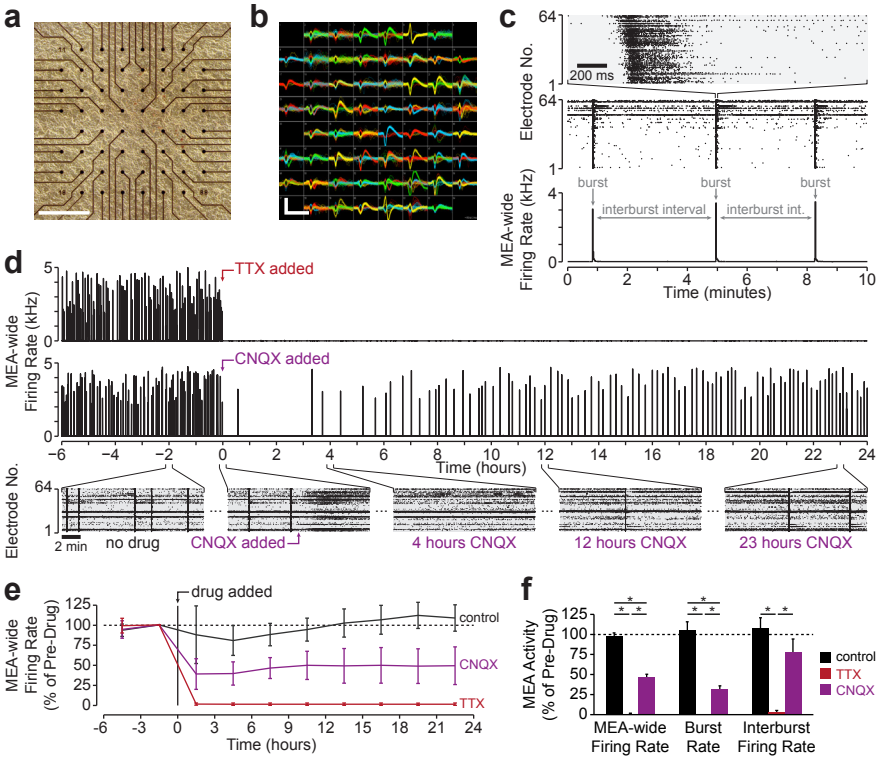

Figure 1: Spiking persists during blockade of AMPAergic transmission. (a) Phase-contrast micrograph of dissociated cortical culture grown on a planar MEA. Scale bar, 500 um. **(b)** Extracellular spike waveforms recorded on each microelectrode shown in (a). Scale bars, 100 uV , 2 ms. **(c)** *Top*, rastergram of spike times occurring during a network-wide burst, a distinguishing feature of spiking activity in dissociated cortical cultures. Scale bar, 200 ms. *Middle*, rastergram showing multiple bursts over several minutes. *Bottom,* time histogram of spikes occurring across the entire MEA over the same time course shown in middle panel. MEA-wide firing rate at each time point is computed by counting the number of spikes occurring during each bin, and dividing by the bin size. Bin size, 1 s. **(d)** *Top and middle*, MEA-wide firing rates from example recordings before and during application of TTX or CNQX. Bin size, 1s. *Bottom*, rastergrams for 15-minute snippets before or during CNQX treatment. Scale bar, 2 min. **(e)** Mean MEA-wide firing rate over time for all TTX- and CNQX-treated cultures (vehicle-treated controls, n=12 cultures; TTX, n=8 cultures; CNQX, n=13 cultures). Values are normalized to firing rate during 3 hour window before drug application. Bin size, 3h. Error bars denote s.d. **(f)** Mean MEA-wide firing rate, burst rate, and interburst firing rate for vehicle-, TTX-, or CNQX-treated cultures during the 24-hour treatment window. Values are normalized to firing rate during 3-hour window before drug application. MEA-wide firing rate was significantly different between all conditions (control, 97.34±4.55%; TTX, 1.11±0.51%; CNQX, 46.20±4.12%; Kruskal-Wallis, $p<10^{-6}$), with TTX being significantly less than both control and CNQX (both $p<10^{-3}$), and CNQX being less than control ($p<10^{-4}$) but greater than TTX. Burst rates followed a similar trend (control, 105.83±9.95%; TTX, 0±0%; CNQX, 31.18±4.76%; Kruskal-Wallis, $p<10^{-6}$; control vs. TTX, $p<10^{-3}$; control vs. CNQX, $p<10^{-4}$, TTX vs. CNQX, $p<10^{-3}$). Firing rate between bursts were also different between conditions (control, 108.12±12.72%; TTX, 3.60±1.50%; CNQX, 108.12±12.72%; Kruskal-Wallis, $p<10^{-4}$), again with TTX reduced compared to both control ($p<10^{-4}$) and CNQX ($p<10^{-4}$), and showing only a mild reduction compared to control ($p=0.02$, not significant at Bonferroni adjusted alpha=0.017). Error bars denote s.e.m.

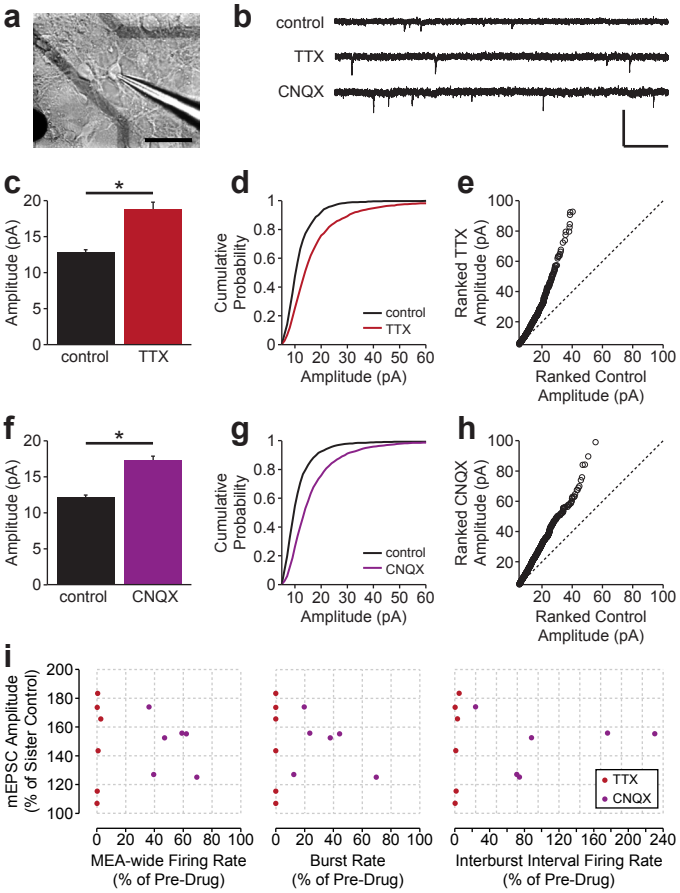

Figure 2: Spiking is not correlated to the magnitude of synaptic scaling. (a) Pyramidal cell during whole-cell recording. Micro-electrode (black, lower left) and electrode leads (grey) are visible. Scale bar, 50 um. **(b)** Sample mEPSC recordings following 24-hour treatment with vehicle, TTX, or CNQX. Scale bar, 50 pA, 200 ms. **(c)** Mean mEPSC amplitude for 6 sister culture pairs treated with vehicle or TTX (control: 12.82±0.36 pA, n=47 cells; TTX: 18.82±1.02 pA, n=58 cells; $p<10^{-5}$). Error bars denote s.e.m. **(d)** Cumulative distribution of mEPSC amplitudes following TTX or vehicle treatment. Multiplicatively scaled TTX distribution matches control ($p>0.6$). **(e)** Ranked TTX mEPSC amplitudes plotted against ranked control amplitudes (linear fit, $R^2 = 0.975$). Dotted line denotes the line of identity. **(f)** Mean mEPSC amplitude for 10 sister culture pairs treated with vehicle or CNQX (control: 12.1±0.34pA, n=89 cells; CNQX, 17.31±0.54pA, n=94 cells; $p<10^{-12}$). **(g)** Cumulative distribution of mEPSC amplitudes following CNQX or vehicle treatment. Multiplicatively scaled CNQX distribution matches control ($p>0.9$). **(h)** Ranked CNQX mEPSC amplitudes plotted against ranked control amplitudes (linear fit, R^2=0.996). **(i)** *Left*, Mean mEPSC amplitude for individual cultures plotted against the firing rate they exhibited during TTX or CNQX treatment. mEPSC amplitudes are normalized to corresponding sister control cultures, and MEA-recorded activity is normalized to pre-drug levels. *Center and right*, Mean mEPSC amplitude plotted against burst rate and interburst firing rate, respectively. (linear fits: MEA-wide firing rate, r=-0.0466; burst rate, r=-0.1136, interburst firing rate, r=0.0435).

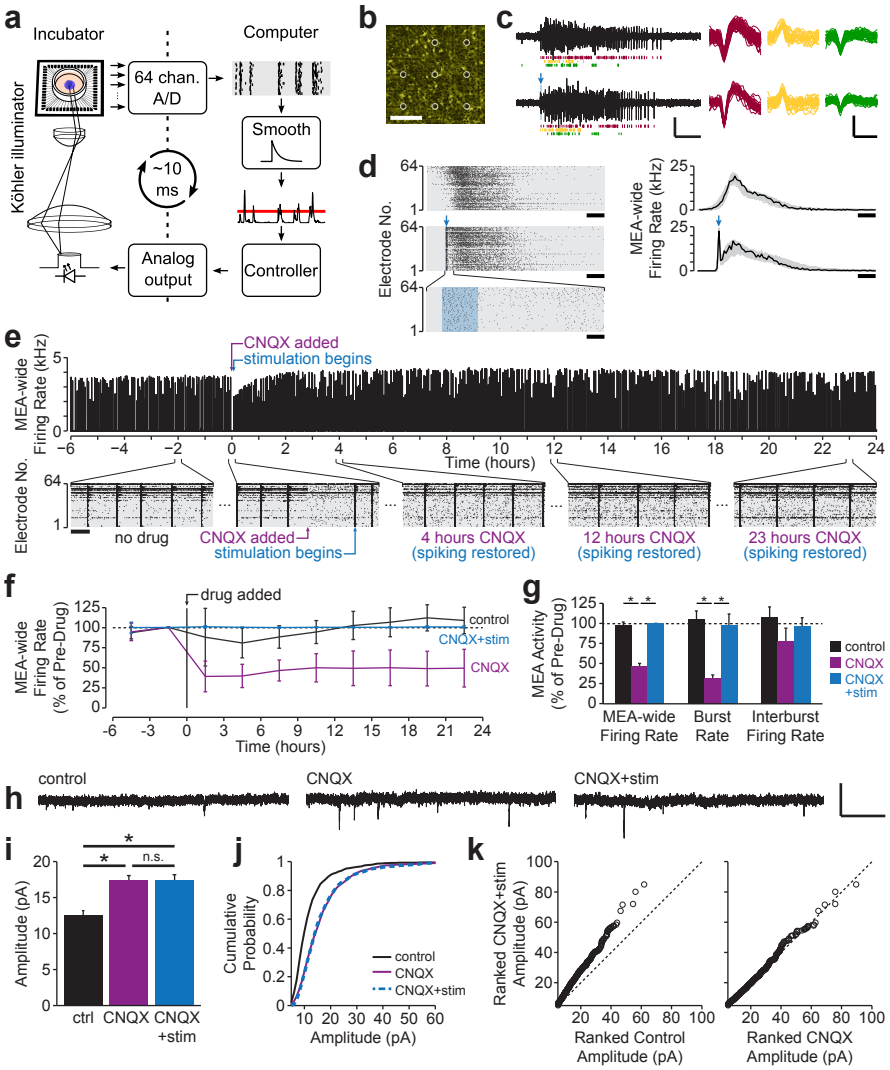

Figure 3: Reduced AMPAergic transmission directly triggers upward synaptic scaling. (a) Schematic of closed-loop optical stimulation system. **(b)** Neurons transfected with ChR2-eYFP. Microelectrodes are circled in white. Scale bar, 200 um. **(c)** *Left*, voltage traces recorded from a single microelectrode during a spontaneous burst in the absence of any drug (top) and a photostimulation-evoked burst in the presence of CNQX (bottom) from the same culture. Blue arrow denotes the timing of the light pulse. Shaded blue bar denotes 10-ms duration of the light pulse, which is brief compared to the total burst duration. Colored vertical bars below each trace denote the spike times for sorted extracelluar units on this microelectrode.Vertical colored bars denote spike times for individual extracellular units. The pattern of recruitment of units is similar between the two conditions. Scale bars, 50 uV, 200 ms. *Right,* extracellular units detected during the bursts shown on the left. Similarity between the spike waveforms across the two conditions indicate that they are likely from the same neurons. Scale bars, 50 uV, 1 ms. **(d)** *Left*, rastergram showing spike times recorded across all electrodes during a spontaneous burst (top) and a photostimulation-evoked burst in the presence of CNQX (middle). The recruitment of spikes across the entire MEA is similar between the two conditions. Blue arrow denotes the timing of the light pulse. Blue shading denotes when light is on, and grey shading indicates when light is off. Zoomed time scale of the CNQX+photostimulation condition (bottom) shows directly evoked spike times. Scale bars, 100 ms (top and middle), 5 ms (bottom). *Right*, MEA-wide firing rate computed during bursts shown at left (black lines). The 107 bursts that occurred during a 6-hour spontaneous recording (top) or the 416 bursts the 24-hour CNQX+photostimulation recording for this culture (bottom) are plotted in grey. Blue arrow denotes timing of the light pulse. Following the direct activation, the firing rates between the spontaneous and CNQX-+photostimulation conditions appear similar. Bin size, 10 ms. Scale bar, 100 ms. **(e)** *Top*, MEA-wide firing rates from example recordings before and during application of CNQX, with pre-CNQX firing rates restored using closed-loop photostimulation. The closed-loop controller begins 5 min after CNQX is added to verify that the drug has taken effect. Bin size, 1s. *Bottom*, rastergrams for 15-minute snippets before or during CNQX and photostimulation. Scale bar, 2 min. **(f)** Mean MEA-wide firing rate over time for CNQX-treated cultures with restored spiking (n=5 cultures). Control and CNQX values from Fig. 1e are shown for comparison. Closed-loop stimulation effectively locked firing rate to pre-CNQX levels. Bin size, 3h. Error bars denote s.d. **(g)** Mean MEA-wide firing rate, burst rate, and interburst firing rate for the 3 conditions during the 24-hour treatment window. CNQX-treated cultures with restored spiking showed no change in MEA activity (MEA-wide firing rate, 100.23±0.41%, p<xx; burst rate, 97.7±31.97%, p<xx; interburst firing rate, 96.21±24.93%, p<xx). Error bars denote s.e.m. **(h)** Sample mEPSC recordings following 24-hour treatment with vehicle, CNQX, or CNQX+photostimulation. Scale bar, 30 pA, 200 ms. **(i)** Mean mEPSC amplitude for 5 sister culture pairs from the 3 treatment conditions (control: 12.64±0.56 pA, n=44 cells; CNQX: 17.38±0.70 pA, n=51 cells; CNQX+photostimulation: 17.43±0.77 pA, n=46 cells; ANOVA, $p<10^{-58}$; control vs. CNQX, $p<10^{-5}$; control vs. CNQX+-photostimulation, $p<10^{-5}$, CNQX vs. CNQX+photostimulation, p>0.9). Error bars denote s.e.m. **(d)** Cumulative distribution of mEPSC amplitudes following the 3 treatment conditions. Multiplicatively scaled CNQX and CNQX+photostimulation distributions matched control (p>0.9 for both), and there was no difference between the unscaled CNQX and CNQX+photostimulation distributions (p>0.9). **(e)** Ranked CNQX+photostimulation mEPSC amplitudes plotted against ranked control or CNQX amplitudes (linear fits, $R^2 = 0.998$ and $R^2 = 0.995$, respectively). Dotted line denotes the line of identity.

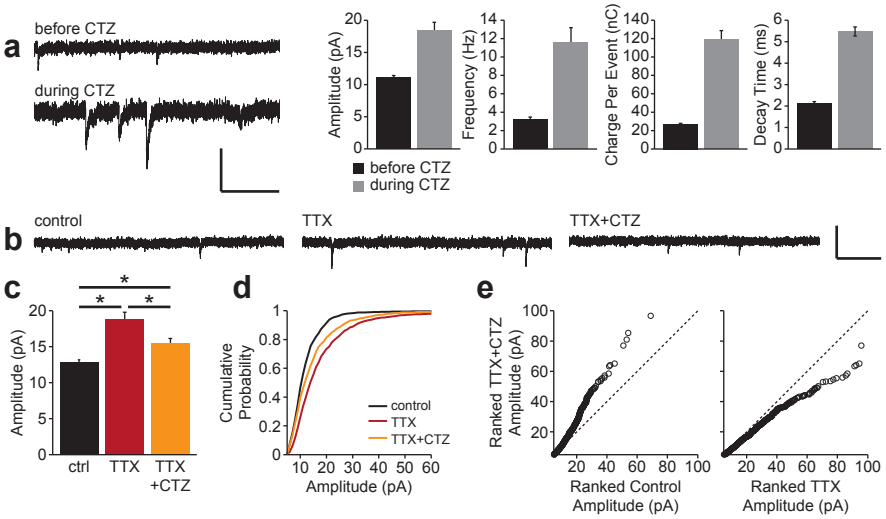

Figure 4: Reduced AMPA receptor activation mediates TTX-induced synaptic scaling. (a) *Left,* sample AMPAergic mEPSCs recorded before and after during CTZ. Scale bar, 25 pA, 200 ms. *Right,* Mean mEPSC amplitude, frequency, charge per event, and decay time constant before and during CTZ. **(b)** Sample mEPSC recordings following 24-hour treatment with vehicle, TTX, or CTZ. Scale bar, 30 pA, 200 ms. **(c)** Mean mEPSC amplitude for 6 sister culture pairs treated from the 3 treatment conditions (control: 12.82±0.36 pA, n=47 cells; TTX: 18.82±1.02 pA, n=58 cells; TTX+CTZ: 15.45±0.69 pA, n=50 cells; ANOVA, $p<10^{-52}$; control vs. TTX, $p<10^{-5}$; control vs. TTX+CTZ, $p<10^{-2}$, TTX vs. TTX+CTZ, $p>10^{-2}$). Error bars denote s.e.m. **(d)** Cumulative distribution of mEPSC amplitudes following the 3 treatment conditions. Multiplicatively scaled TTX and TTX+CTZ distribution match control ($p>0.7$ and $p>0.5$, respectively), and there is a significant difference between the unscaled TTX and TTX+CTZ distributions ($p< 10^{-6}$). **(e)** Ranked TTX+CTZ mEPSC amplitudes plotted against ranked control or TTX amplitudes (linear fits, $R^2 = 0.990$ and $R^2 = 0.989$, respectively). Dotted line denotes the line of identity.

Supplementary Methods (some of these will be ported to methods section in main text)

Cell culture

Primary cultures of neurons and glia were derived from E18 rat neocortex and grown on polyethylenimine- and laminin-coated microelectrode arrays (Multichannel Systems 60MEA200/30ir-Ti-pr) or glass bottom dishes (P35G-1.5-10-C) as described in Hales et al., 2010. Growth medium contained: 90% high-glucose DMEM, 10% horse serum, 0.5mM GlutaMAX, 1mM sodium pyruvate, 2.5ug/mL insulin (pH 7.2, 315 mOsm). Incubator was regulated at at 35°C and 5% CO2. Cultures were transfected with AAV9-hSynapsin-ChR2(H134R)-eYFP (from Dr. Karl Deisseroth via the University of Pennsylvania Vector Core) at 1 day in vitro. The following drug concentrations were used: TTX, 1uM; CNQX, 40uM; bicuculline, 20uM; cyclothiazide, 100uM. DMSO or water was used as vehicle, corresponding to the stable solvent used to dilute the drug that sister cultures were treated with. All experiments were performed during the second week *in vitro*.

Microelectrode array (MEA) recordings

MEA recordings were performed in standard growth medium in the cell culture incubator. Extracellular voltage waveforms were continuously sampled at 25kHz using the Neurorighter acquisition system (Newman et al., 2012, Rolston et al., 2009). Voltage recordings were filtered with a 3rd order Butterworth bandpass at 200-3000Hz, and action potentials were detected at threshold of ±5 times the root mean square error. Analysis of spike data was performed in MATLAB (The Mathworks). The pre-drug

period was defined as a 3-hour segment preceding TTX, CNQX, or vehicle application. The treatment period was defined as the entire 24 hours during TTX, CNQX, or vehicle application. After the treatment period, all drugs were washed 4 times with standard growth medium.

Whole-cell recordings

Miniature excitatory postsynaptic currents (mEPSCs) were recorded from pyramidal-shaped cells in a continuous perfusion of artificial cerebrospinal fluid containing (in mM): 126 NaCl, 3 KCl, 2 $CaCl_2$, 1.5 $MgSO_4$, 1 NaH_2PO_4, 25 $NaHCO_3$, and 25 D-glucose, and saturated with 95% O2 and 5% CO2 (pH 7.4, 315 mOsm). To isolated AMPAergic mEPSCs, solution was supplemented with containing 1μM TTX and 20μM bicuculline. Temperature was regulated at 35°C using an inline heater (Warner ???). Internal solution contained (in mM): 100 K-gluconate, 30 KCl, 10 HEPES, 2 MgSO4, 0.5 EGTA, 3 ATP (pH 7.4, 290 mOsm). mEPSCs were recorded using an EPC8 amplifier (HEKA). mEPSCs were analyzed, blind to the treatment condition, using MiniAnalysis (Synaptosoft). Pipette resistances were 2-8Mohms. mEPSCs with amplitudes <5pA were excluded from analysis.

Optical stimulation

To deliver optical stimuli, a custom N-channel enhancement mode MOSFET current source (https://potterlab.gatech.edu/main/newman/wiki/index.php?title=Cyclops_Driver_R2) was used to drive a blue LED (46511 nm FWHM;

LZ4-00B200, LEDEngin, San Jose, CA). The LED was butt-coupled to a randomized fiber bundle (Schott AG, Mainz, Germany) which fed light to a Köhler illumination train mounted beneath the MEA amplifier. A full description and characterization of the closed-loop optical stimulation system used in this study is given in (Newman et al., 2013). Briefly, the average network firing rate was calculated every dt = 10 ms according to

$$f[t] = r[t] + (1 - \alpha) f[t - dt]$$

where = 5 sec/dt and and $r[t]$ = no. detected spikes/dtis the instantaneous firing at time t. The target rate, f^*, was defined as $f[t]$ averaged over a 3 hour period prior to CNQX application. Five minutes following the application of CNQX to the culturing medium, an error signal was generated between the target and measured firing rate according to

$$e_f[t] = f^* - f[t].$$

Finally, an on-off controller was used to determine stimulus application according to

$$if \sum_t e_f[t] > 0, \text{ apply } 10 \text{ ms pulse.}$$

(note: currently there's no way to notate summations properly in Pages; I will correct this when we port the document to a more supportive text editor)

Each stimulus pulse resulted in uniformly distributed 10.1 mW/mm^2 light the plane of the culture. The rise and fall times of each LED pulse were ~10 µs.

References for Supplementary Methods

Hales CM, Rolston JD, Potter SM (2010) How to culture, record and stimulate neuronal networks on micro-electrode arrays (MEAs). Journal of visualized experiments : JoVE:1–7.

Newman JP, Zeller-Townson R, Fong M-F, Arcot Desai S, Gross RE, Potter SM (2012) Closed-loop, multichannel experimentation using the open-source NeuroRighter electrophysiology platform. Frontiers in Neural Circuits 6:98.

Newman JP, Fong M-F, Potter SM (2013) Optogenetic feedback control of neuronal firing. Submitted

Rolston JD, Gross RE, Potter SM (2009) A low-cost multielectrode system for data acquisition enabling real-time closed-loop processing with rapid recovery from stimulation artifacts. Frontiers in Neuroengineering 2:1-17.

List of Supplementary Figures

Supplementary Fig. 1: Computing firing rates, identifying bursts, etc

- show how bursts and interburst intervals were identified

Supplementary Fig. 2: mEPSC frequency and decay kinetics for TTX and CNQX

- bar charts comparing other mEPSC features

Supplementary Fig. 3: Optogenetic stimulation during CNQX treatment effectively mimics spontaneous bursts.

- Stimulation on all 59-channels for spontaneous vs. in CNQX
- Raster plot for snippets shown in (a)
- correlation plots for pre and post drug for CNQX vs. CNQX+stim

Supplementary Fig. 4: NMDAergic transmission is responsible for long-latency spiking during evoked stimulation.

(a) Chronic CNQX eliminates bursts, and when they recover they contain long-latency component, similar to spontaneous pre-drug bursts. (6-well)

(b) Chronic APV alone eliminates bursts, and when they recover contain are shorter than spontaneous pre-drug bursts. (6-well)

(c) APV+CNQX eliminates bursts for days.

(d) Bursts evoked during CNQX alone contain fast and slow components.

(e) Bursts evoked during APV alone contain only fast component. (get from jon)

Supplementary Fig. 5: mEPSC frequency and decay kinetics for CNQX and CNQX +stim

- bar charts comparing other mEPSC features

Supplementary Fig. 6: Cyclothiazide is effective at enhancing quantal AMPAR activation for at least 12 hours.

- bar chart showing amplitude, frequency, decay, charge for pre-drug, 0-3hr, 3-6hr, 6-9hr, and 9-12hr
- example mEPSC traces measured at each time point

Supplementary Fig. 7: Cyclothiazide does not change effects of TTX on spiking activity.

- equivalent of Fig. 1d-f and Fig. 3e-g for TTX+CTZ data (it looks the same as TTX only)

Supplementary Fig. 8: mEPSC frequency and decay kinetics for TTX and TTX +CTZ

- bar charts comparing other mEPSC features